NACA RM A56G19

NACA

RESEARCH MEMORANDUM

WIND-TUNNEL TESTS OF BLOWING BOUNDARY-LAYER CONTROL WITH JET PRESSURE RATIOS UP TO 9.5 ON THE TRAILING-EDGE FLAPS OF A 35° SWEPTBACK WING AIRPLANE

By Mark W. Kelly and Jeffrey H. Tucker

Ames Aeronautical Laboratory
Moffett Field, Calif.

NATIONAL ADVISORY COMMITTEE
FOR AERONAUTICS

WASHINGTON

October 26, 1956
Declassified July 26, 1957

NATIONAL ADVISORY COMMITTEE FOR AERONAUTICS

RESEARCH MEMORANDUM

WIND-TUNNEL TESTS OF BLOWING BOUNDARY-LAYER CONTROL WITH JET PRESSURE RATIOS UP TO 9.5 ON THE TRAILING-EDGE FLAPS OF A 35° SWEPTBACK WING AIRPLANE

By Mark W. Kelly and Jeffrey H. Tucker

SUMMARY

A full-scale wind-tunnel investigation was made to determine whether the effects of blowing high-velocity air over trailing-edge flaps could be adequately correlated by the jet momentum over a wide range of jet velocities (i.e., jet pressure ratios from subcritical to 9.5). The model selected for these tests was a 35° sweptback wing airplane which had been equipped with plain flaps having blowing boundary-layer control. Three-component force data and flow and pressure ratio requirements of the blowing boundary-layer control system were obtained at Reynolds numbers of 7.6×10^6 and 10.7×10^6.

Good correlation of lift with jet momentum was obtained over the above range of jet pressure ratios.

INTRODUCTION

It has been experimentally demonstrated in many previous investigations that large increases in lift at low speeds may be obtained by ejecting high-velocity air over wing trailing-edge flaps (e.g., refs. 1 through 4). The results of most of these investigations indicate that the increase in lift obtained by using blowing boundary-layer control is primarily a function of the momentum of the air ejected over the flap. This means that it should be possible to obtain the same increase in flap effectiveness with either high mass flows and low jet velocities or low mass flows and high jet velocities, as long as the momentum of the jet is not changed. This is of considerable practical importance for two reasons: (1) it indicates that the flow and pressure ratio requirements of a blowing boundary-layer control system can be satisfied by a wide variety of pumping systems and (2) it means that the amount of wind-tunnel testing is

considerably reduced and simplified since it is not necessary to duplicate the flows and pressure ratios of all pumping systems that might be of practical importance.

In the investigations reported in references 1 and 2, it was found that the increase in flap effectiveness due to blowing could be correlated, within experimental accuracy, with the jet momentum over a range of jet pressure ratios from subcritical to 4.6. (The jet pressure ratio is defined as the ratio of total pressure in the duct ahead of the flap nozzle to free-stream static pressure.) However, as pointed out in references 3 and 4, this degree of correlation has not always been obtained.

At the present time, blowing boundary-layer control systems are being considered on a number of airplanes having high performance engines which are capable of providing air to the boundary-layer control system at pressure ratios of the order of 10. This is roughly two to three times the maximum pressure ratios utilized in the investigations of references 1 and 2. Since the justification for using the jet momentum as the primary design parameter is largely empirical, it was believed advisable to investigate in the wind tunnel the performance of a blowing boundary-layer control system using pressure ratios of about 10.

The specific purpose of this investigation was to determine experimentally whether the effectiveness of a blowing-flap installation could be specified over a wide range of jet pressure ratios by the momentum of the jet. An F-93 airplane which had been equipped with a J-57 engine and blowing boundary-layer control flaps was utilized as a model for this investigation. The tests covered a range of jet pressure ratios from subcritical to 9.5 and were conducted at Reynolds numbers of 7.6×10^6 and 10.7×10^6.

NOTATION

A	area, sq ft
b	wing span, ft
c	wing chord parallel to plane of symmetry, ft
$\bar{c}$	mean aerodynamic chord, $\dfrac{\int_0^{b/2} c^2 dy}{\int_0^{b/2} c\, dy}$
C	thrust coefficient of tailpipe

C_D drag coefficient, $\frac{\text{drag}}{q_\infty S}$

C_L lift coefficient, $\frac{\text{lift}}{q_\infty S}$

ΔC_L increment of lift coefficient due to flaps

C_m pitching-moment coefficient, $\frac{\text{pitching moment}}{q_\infty S\bar{c}}$

C_Q flow coefficient, $\frac{W_j}{wU_\infty S}$

C_μ momentum coefficient, $\frac{W_j/g}{q_\infty S} V_j$

$C_{L_{\delta_1}}$ rate of change of lift coefficient with flap deflection for full wing-chord flap (given as $C_{L_{\delta_1}}$ in ref. 6)

d distance from engine thrust line to moment center, positive when thrust line is above moment center, ft

$\frac{d\alpha}{d\delta_f}$ flap lift-effectiveness parameter

F_G gross thrust from engine, $\frac{W_E V_{TP}}{g}$, lb

g acceleration of gravity, 32.2 ft/sec^2

h_s nozzle height, in.

p static pressure, lb/sq ft

p_t total pressure, lb/sq ft

p_d total pressure in flap duct, lb/sq ft

q dynamic pressure, lb/sq ft

R Reynolds number, $\frac{U_\infty \bar{c}}{\nu}$; or gas contstant for air, 1716 sq ft/sec^2 $^\circ$R

S wing area, sq ft

S_f wing area spanned by flaps, sq ft

T temperature, $^\circ$R

U velocity, ft/sec

V_j jet velocity assuming isentropic expansion, $\sqrt{\frac{2\gamma}{\gamma-1} RT_d \left[1 - \left(\frac{p_\infty}{p_d}\right)^{\frac{\gamma-1}{\gamma}}\right]}$, ft/sec

V_{TP} velocity at exit of engine tailpipe, ft/sec

W weight rate of flow, lb/sec

w specific weight of air at standard conditions, 0.0765 lb/cu ft

x distance along airfoil chord normal to wing quarter-chord line, in.

y spanwise distance perpendicular to plane of symmetry, ft

z height in inches above wing reference plane defined by quarter-chord line and the chord of the wing section at $0.663 \frac{b}{2}$

Λ sweep angle, deg

α angle of attack of fuselage reference line, deg

δ_f flap deflection, measured normal to flap hinge line (given as $\underline{\delta}$ in ref. 6), deg

$\underline{\delta}_f$ flap deflection, measured in a plane parallel to the plane of symmetry (given as δ in ref. 6), deg

ν kinematic viscosity of air, ft^2/sec

γ ratio of specific heats, for air 1.4

Subscripts

d trailing-edge flap duct

E engine

f trailing-edge flaps

j flap jet

max maximum

t total

u	uncorrected
TD	engine turbine discharge
TP	engine tailpipe
∞	free stream

MODEL AND APPARATUS

Model

The model consisted of an F-93 airplane on which the normal single-slotted flaps had been replaced by blowing boundary-layer-control flaps similar to those used in the investigation reported in reference 1. In order to obtain the desired high jet pressure ratios, a J-57 turbojet engine was installed in the airplane. Since the existing side inlets were not adequate to supply the air flow required by this engine, the front end of the fuselage was modified to allow a nose inlet to be installed.

A photograph of the model installed in the Ames 40- by 80-foot wind tunnel is shown in figure 1. The major dimensions of aerodynamic importance are shown in figure 2. The coordinates of the wing airfoil sections are given in table 1. Details of the wing and flaps are shown in figure 3. The chordwise location of the nozzle shown in figure 3 was used throughout the tests. This particular location is the same as that used for most of the investigation presented in reference 1, and was chosen to afford direct comparison of those results with the data presented herein. Static-pressure orifices were installed in the flap upper surface so that the degree of flow separation could be estimated. Measurements of the nozzle opening across the span of the flaps are presented in figure 4. These measurements were all taken with no flow through the nozzle and with the nozzle at ambient temperature. However, it is believed that the nozzle opening did not change significantly under load, since the upper and lower nozzle blocks were rigidly secured with screws and 0.25-inch wide spacers at 3-1/4-inch intervals.

Instrumentation

Measurements to obtain C_μ.- The weight rate of flow of air delivered to each flap was measured by a three-quarter radius flowmeter (ref. 5) installed in the bleed air ducting near the root of each flap. The flowmeter with ducting was calibrated against a standard thin plate orifice. The total pressures and temperatures needed to compute the jet momentum were also measured near the flap root. Additional pressure and temperature measurements were made near the flap tip to make sure that the jet velocity was uniform along the span of the flap.

Measurement of engine thrust.- The gross thrust of the engine was obtained from measurements of the turbine discharge total pressure as discussed in the section entitled "Engine Thrust Calibration." These pressure measurements were made with the total pressure probes furnished with the engine. The weight rate of flow through the engine, required for computation of ram drag, was obtained from turbine discharge total-pressure and total-temperature measurements.

TESTS

Range of Variables

The investigation covered a range of momentum coefficients from zero to 0.022, and of flap jet pressure ratios from subcritical up to 9.5. In order to utilize this range of pressure ratios, the flap nozzle openings were changed from 0.042 to 0.006 inch. The model was tested with flap deflections of 0°, 45°, and 60°, and at Reynolds numbers of 7.6×10^6 and 10.7×10^6 based on the mean aerodynamic chord (8.22 feet). These Reynolds numbers correspond to free-stream dynamic pressures of 25 and 50 pounds per square foot, respectively. All tests were made with the horizontal tail off. The leading-edge slats were retracted but not sealed throughout the test except for one run made to investigate the effect of sealing the slat-wing juncture.

Method of Testing

Aerodynamic data.- The variation of C_L with C_μ at angles of attack below the stall was determined by varying C_μ at angles of attack of 0° and 8°. The effects of blowing on $C_{L_{max}}$ were determined by pitching the model through the stall with various constant values of momentum coefficient. The additional information required to obtain typical lift, drag, and pitching-moment data for the model was obtained by testing at several other angles of attack with a constant jet momentum well above that required to attach the flow on the flap.

Engine thrust calibration.- The gross thrust of the engine was computed from measurements of turbine discharge total pressure by the following equation:

$$F_G = CA_{TP}\left\{\frac{2\gamma}{\gamma-1}\,p_{TP}\left[\left(\frac{p_{t_{TD}}}{p_{TP}}\right)^{\frac{\gamma-1}{\gamma}} - 1\right] + \left(p_{TP} - p_\infty\right)\right\}$$

When the engine was operating with the tailpipe choked, it was assumed that the jet static pressure at the tailpipe exit was equal to $[(\gamma+1)/2]^{\frac{-\gamma}{\gamma-1}} p_{t_{TD}}$. When the tailpipe was not choked, it was assumed that the jet static pressure was equal to free-stream static pressure. The nozzle thrust coefficient was evaluated by solving for C in the above equation with values of F_G determined from wind-tunnel balance measurements. It was not possible to directly measure F_G with the wind-tunnel balance system since operation of the engine at high thrust induced a flow of about 80 feet per second in the wind-tunnel test section. The values of F_G used to obtain the thrust coefficient C were obtained by correcting the measured thrust for airplane drag and inlet ram drag by the following equation:

$$F_G = \text{Measured Thrust} + C_D q_\infty S + \frac{W_E}{g} U_\infty$$

The thrust calibration was made at a free-stream dynamic pressure of 10 pounds per square foot. The drag coefficient was obtained from engine-off tests at the same tunnel speed. (It is recognized that the drag coefficient of the airplane with the engine operating may not be the same as with the engine off. However, the total drag of the airplane at a dynamic pressure of 10 pounds per square foot is only a small percentage of the engine thrust, and any effects of changes in drag coefficient on the computed gross thrust should be negligible.)

The weight rate of flow through the engine was computed from turbine discharge measurements using the following equation:

$$W_E - W_j = gAp_{TP} \sqrt{\frac{2}{RT_{t_{TP}}} \left(\frac{\gamma}{\gamma-1}\right) \left(\frac{p_{t_{TD}}}{p_{TP}}\right)^{\frac{\gamma-1}{\gamma}} \left[\left(\frac{p_{t_{TD}}}{p_{TP}}\right)^{\frac{\gamma-1}{\gamma}} - 1\right]}$$

As in the computation for F_G, it was assumed that, when the tailpipe was choked, the jet static pressure at the nozzle exit was equal to $[(\gamma+1)/2]^{\frac{-\gamma}{\gamma-1}} p_{t_{TD}}$. When the tailpipe was not choked, it was assumed that the jet static pressure was equal to free-stream static pressure. In addition, the above computation assumes that the nozzle coefficient is equal to 1.0.

CORRECTIONS

Effects of Wind-Tunnel Walls

The following corrections for the effects of wind-tunnel wall interference were made:

$$\alpha = \alpha_u + 0.639\ C_{L_u}$$

$$C_D = C_{D_u} + 0.0112\ C_{L_u}^2$$

$$C_m = C_{m_u}$$

Effects of Engine Operation

The force data obtained from the wind-tunnel balance system were corrected for the effects of engine thrust as follows:

$$C_L = \frac{\text{total lift}}{q_\infty S} - \frac{F_G}{q_\infty S} \sin \alpha$$

$$C_D = \frac{\text{total drag}}{q_\infty S} + \frac{F_G}{q_\infty S} \cos \alpha - \frac{W_E U_\infty}{g q_\infty S}$$

$$C_m = \frac{\text{total moment}}{q_\infty \bar{c} S} + \frac{F_G}{q_\infty S} \frac{d}{\bar{c}} - \frac{W_E U_\infty}{g q_\infty S} \left(\frac{d}{\bar{c}} \cos \alpha + \frac{l}{\bar{c}} \sin \alpha \right)$$

These corrections include the force on the inlet duct due to turning the air when the airplane is at an angle of attack. The distance, l, from the moment center to the point in the inlet duct at which this force may be considered to act, was obtained by solving the above moment equation for $l/\bar{c}$ with values of C_m obtained from engine-off tests.

RESULTS AND DISCUSSION

Correlation of Momentum Coefficient With Flap Effectiveness

The variation of C_L with C_μ, p_d/p_∞, and C_Q is shown in figures 5 and 6. These data were obtained from a series of tests in which the model

configuration was not changed except for the size of the jet nozzle opening, h_s, which was reduced from 0.042 inch to 0.006 inch. (These values of h_s correspond to values of h_s/c from 0.00042 to 0.00006, respectively.) The data presented in figures 5(a) and 6(a) indicate that the size of the nozzle opening had no significant effect on the variation of C_L with C_μ. The variation of C_L with p_d/p_∞ and C_Q, presented in figures 5(b), 5(c), 6(b), and 6(c), show that the variation of C_L with p_d/p_∞ and C_Q was, of course, significantly affected by the size of the nozzle. Similar results were obtained in the investigations reported in references 1 and 2. In general, the conclusions stated in reference 1 were not altered by the results of this investigation; that is, no significant effects were obtained on the variation of C_L with C_μ due to increasing the flap jet pressure ratio from the maximum value of 2.9 used in that investigation to 9.5.

Effects of Blowing on the Lift, Drag, and Pitching Moment

Typical effects of blowing over the flaps on the lift, drag, and pitching-moment characteristics of the model are shown in figure 7. These results are similar to those presented in reference 1 with the exception that $C_{L_{max}}$ was lower and the stall was not so abrupt. This was primarily caused by leakage through the leading-edge slat joints which were not sealed for these tests as they were in the investigation reported in reference 1.

Comparison With Other Results

The variation of ΔC_L with C_μ, presented in figure 8, was obtained in this investigation at a Reynolds number of 7.6×10^6 to permit a direct comparison with reference 1. These data show that the ΔC_L for values of C_μ over 0.011 obtained on the model as used in most of the tests (slats not sealed and hatches open) was approximately 0.17 less than that obtained on the F-86D airplane. As shown in figure 8, approximately 0.07 of this difference was due to flow through the open fuselage hatches on the F-93 and to leakage through the slat joints. (The fuselage hatches were left open for most of the tests to aid in engine cooling.) In addition, a difference of about 0.05 in ΔC_L would be expected theoretically because of plan-form differences. (The F-93 wing had the same size flaps but a larger wing than the F-86D.)

Comparison With Theory

Theoretical flap lift increments computed using the theory presented in reference 6 are presented in figure 8 along with the experimentally obtained variation of C_L with C_μ.[1] With the fuselage hatches closed, the experimental ΔC_L at a C_μ of 0.011 is approximately 6 percent below the theoretical value. With these hatches open, the experimental ΔC_L was about 14 percent below theory. Pressure distribution measurements on the flaps indicated that for this C_μ the flow was essentially attached in both cases. It is believed that the differences between theory and experiment for the two airplanes are primarily due to different fuselage effects on the span loading of the wings which are not taken into account in the theory of reference 6. (The F-93 airplane has similar wing panels but a larger fuselage than the F-86D airplane.)

CONCLUSION

The results of this investigation show that the increase in effectiveness of the flaps with blowing boundary-layer control can be correlated with the jet momentum coefficient for jet pressure ratios from subcritical to 9.5.

Ames Aeronautical Laboratory
National Advisory Committee for Aeronautics
Moffett Field, Calif., July 19, 1956

---

[1]The theoretical flap effectiveness was estimated from

$$\Delta C_L = (d\alpha/d\delta_f)\, C_{L_{\underline{\delta}_1}}\, \underline{\delta}_f/57.3 \quad \text{(equivalent to eq. 7, ref. 6)}$$

For the F-93 wing

$C_{L_{\underline{\delta}_f}} = 1.44$ (from cross plot of fig. 5, ref. 6)

$d\alpha/d\delta_f = 0.58$ (from curve for theoretical flap effectiveness, fig. 3, ref. 6. Average flap-chord ratio of 0.23 perpendicular to flap hinge line.)

$\tan \underline{\delta}_f = \cos \Lambda_f \tan \delta_f = 0.895 \tan \delta_f$

$\underline{\delta}_f = 57.2^\circ$ for $\delta_f = 60^\circ$

$\Delta C_L = (0.58)(1.44)(57.2/57.3) = 0.834$

REFERENCES

1. Kelly, Mark W., and Tolhurst, William H., Jr.: Full-Scale Wind-Tunnel Tests of a 35° Sweptback Wing Airplane With High-Velocity Blowing Over the Trailing-Edge Flaps. NACA RM A55I09, 1955.

2. Harkleroad, E. L., and Murphy, R. D.: Two-Dimensional Wind-Tunnel Tests of a Model of an F9F-5 Airplane Wing Section Using a High-Speed Jet Blowing Over the Flap. Part I - Tests of a 6-Foot Chord Model. DTMB Rep. Aero. 845, BuAer, Navy Dept., TED No. TMB DE-3134, May, 1953.

3. Williams, J.: An Analysis of Aerodynamic Data on Blowing Over Trailing Edge Flaps for Increasing Lift. British A.R.C. Performance Sub-committee 17,027, Sept. 6, 1954.

4. Dods, Jules B., and Watson, Earl C.: The Effects of Blowing Over Various Trailing-Edge Flaps on an NACA 0006 Airfoil Section, Comparisons With Various Types of Flaps on Other Airfoil Sections, and an Analysis of Flow and Power Relationships for Blowing Systems. NACA RM A56C01, 1956.

5. Preston, J. H., and Gregory, N.: The Three-Quarter Radius Pitot Tube Type of Flow Meter. British A.R.C. Wind Tunnel Design Committee 12,304, April 21, 1949.

6. DeYoung, John: Theoretical Symmetric Span Loading Due to Flap Deflection for Wings of Arbitrary Plan Form at Subsonic Speeds. NACA Rep. 1071, 1952. (Formerly NACA TN 2278)

TABLE I.- COORDINATES OF THE WING AIRFOIL SECTIONS NORMAL TO THE WING QUARTER-CHORD LINE AT TWO SPAN STATIONS

[Dimensions given in inches]

Section at 0.491 semispan			Section at 0.863 semispan		
	z			z	
x	Upper surface	Lower surface	x	Upper surface	Lower surface
0	0.231	---	0	-0.098	---
.119	.738	-0.307	.089	.278	-0.464
.239	.943	-.516	.177	.420	-.605
.398	1.127	-.698	.295	.562	-.739
.597	1.320	-.895	.443	.701	-.897
.996	1.607	-1.196	.738	.908	-1.089
1.992	2.104	-1.703	1.476	1.273	-1.437
3.984	2.715	-2.358	2.952	1.730	-1.878
5.976	3.121	-2.811	4.428	2.046	-2.176
7.968	3.428	-3.161	5.903	2.290	-2.401
11.952	3.863	-3.687	8.855	2.648	-2.722
15.936	4.157	-4.064	11.806	2.911	-2.944
19.920	4.357	-4.364	14.758	3.104	-3.102
23.904	4.480	-4.573	17.710	3.244	-3.200
27.888	4.533	-4.719	20.661	3.333	-3.250
31.872	4.525	-4.800	23.613	3.380	-3.256
35.856	4.444	-4.812	26.564	3.373	-3.213
39.840	4.299	-4.758	29.516	3.322	-3.126
43.825	4.081	-4.638	32.467	3.219	-2.989
47.809	3.808	-4.452	35.419	3.074	-2.803
51.793	3.470	-4.202	38.370	2.885	-2.574
55.777	3.066	-3.891	41.322	2.650	-2.302
59.761	2.603	-3.521	44.273	2.374	-1.986
[a]63.745	2.079	-3.089	[a]47.225	2.054	-1.625
83.681	-.740	---	63.031	.321	---
Leading-edge radius: 1.202, center at (1.201, 0.216)			Leading-edge radius: 0.822, center at (0.822, -0.093)		

[a]Straight lines to trailing edge

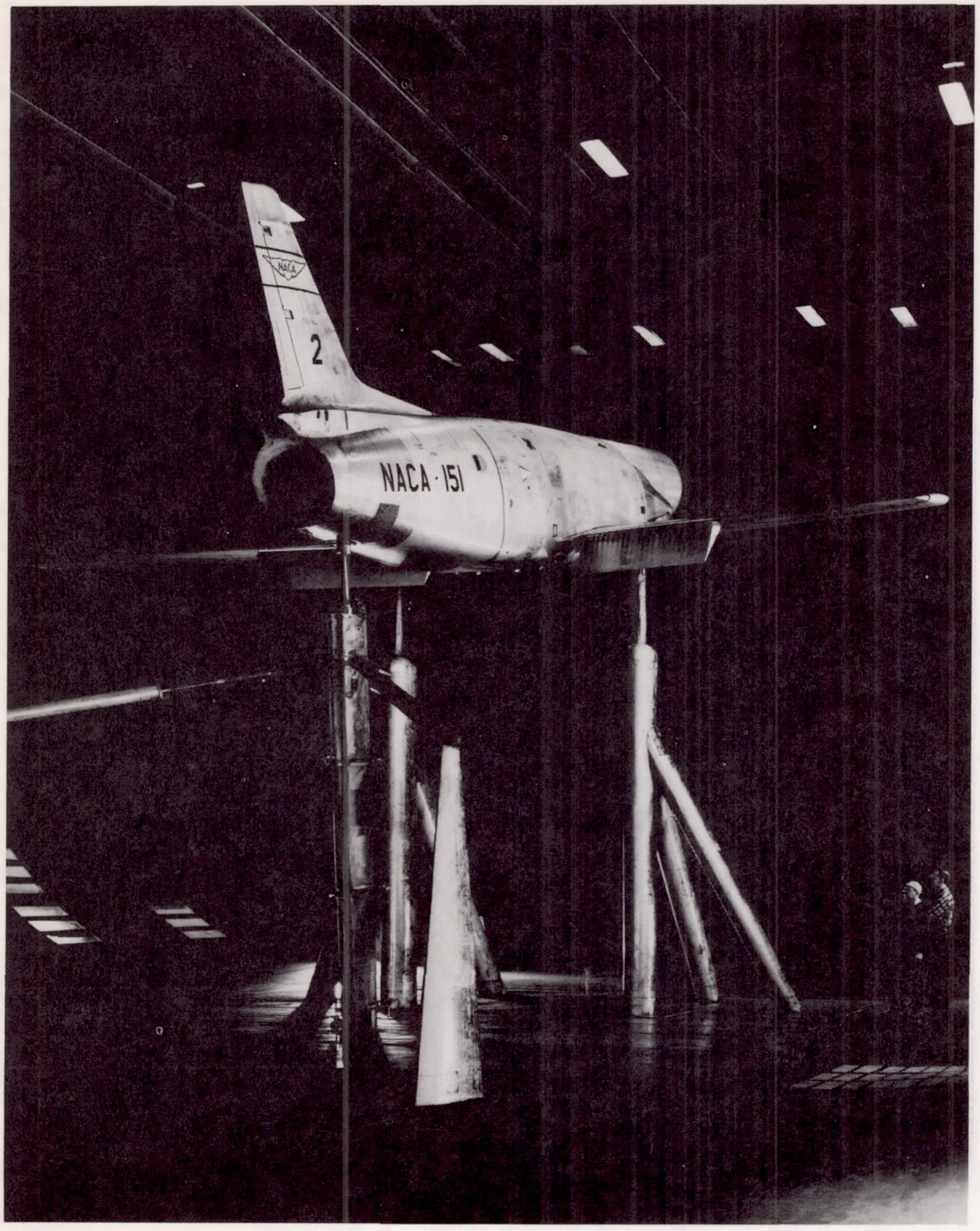

A-21242

Figure 1.- The model mounted in the Ames 40- by 80-foot wind tunnel.

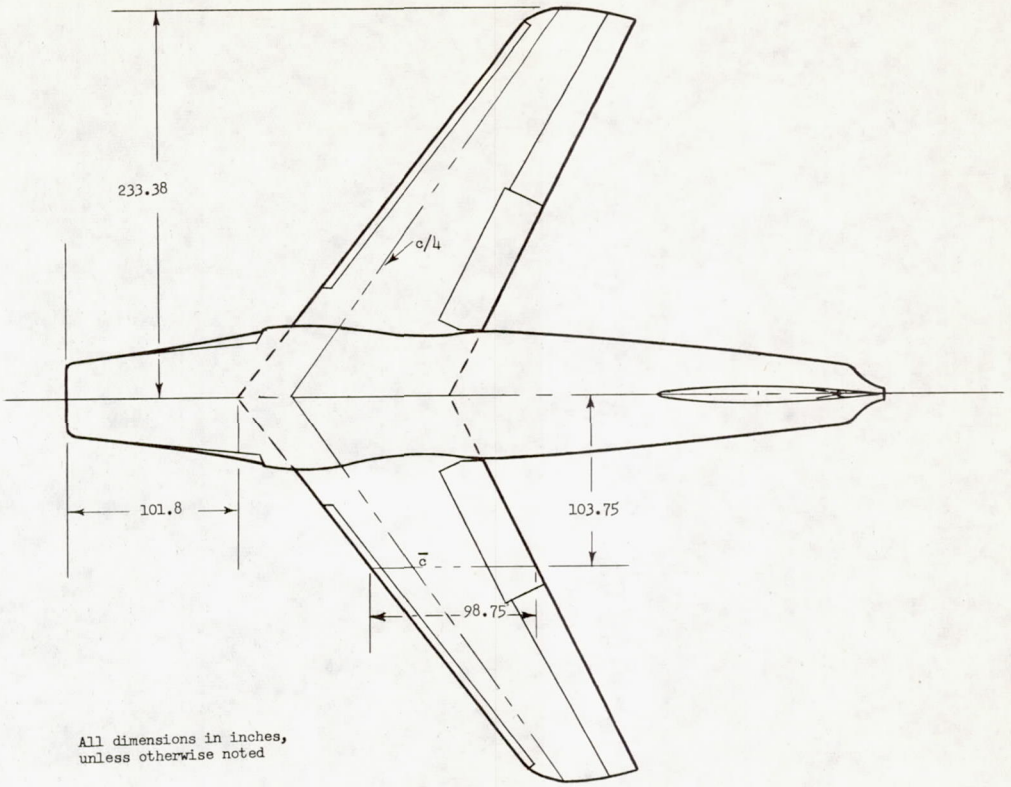

All dimensions in inches, unless otherwise noted

Wing	
Sweep (quarter-chord line)	35.00°
Aspect ratio	4.943
Taper ratio	0.501
Twist	2.0°
Dihedral	1.0°
Area	306.10 sq ft
Incidence (root)	1.0°
Airfoil section (root)	NACA 0012-64 (modified)
Airfoil section (tip)	NACA 0011-64 (modified)
Ratio of wing area spanned by flaps to total wing area (S_f/S)	0.367

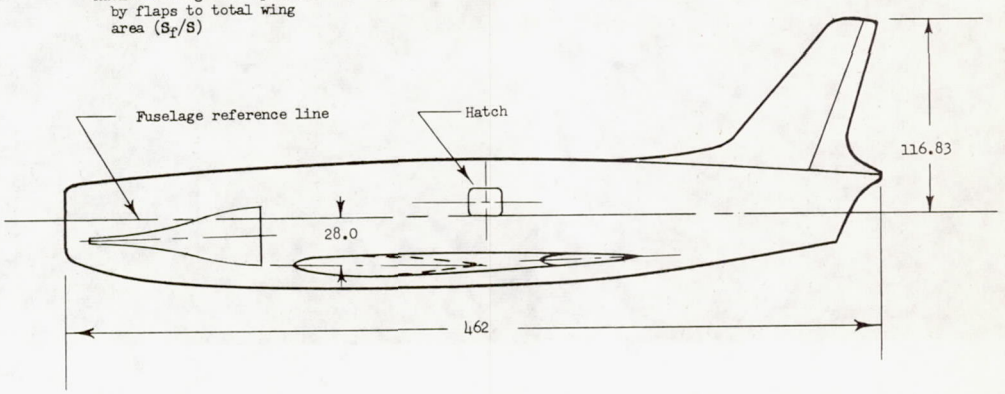

Figure 2.- General arrangement of model.

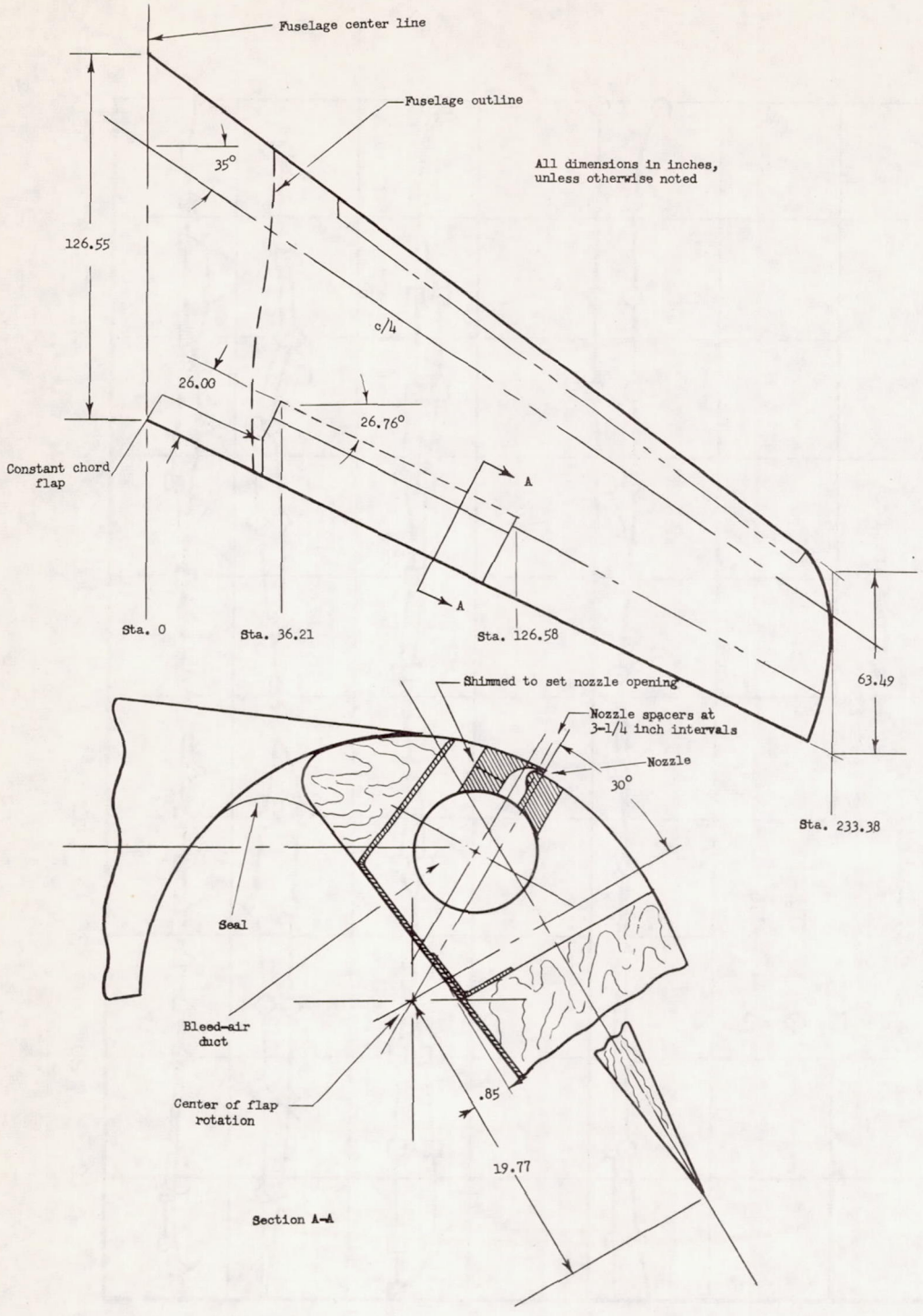

Figure 3.- Details of wing and flap boundary-layer control system.

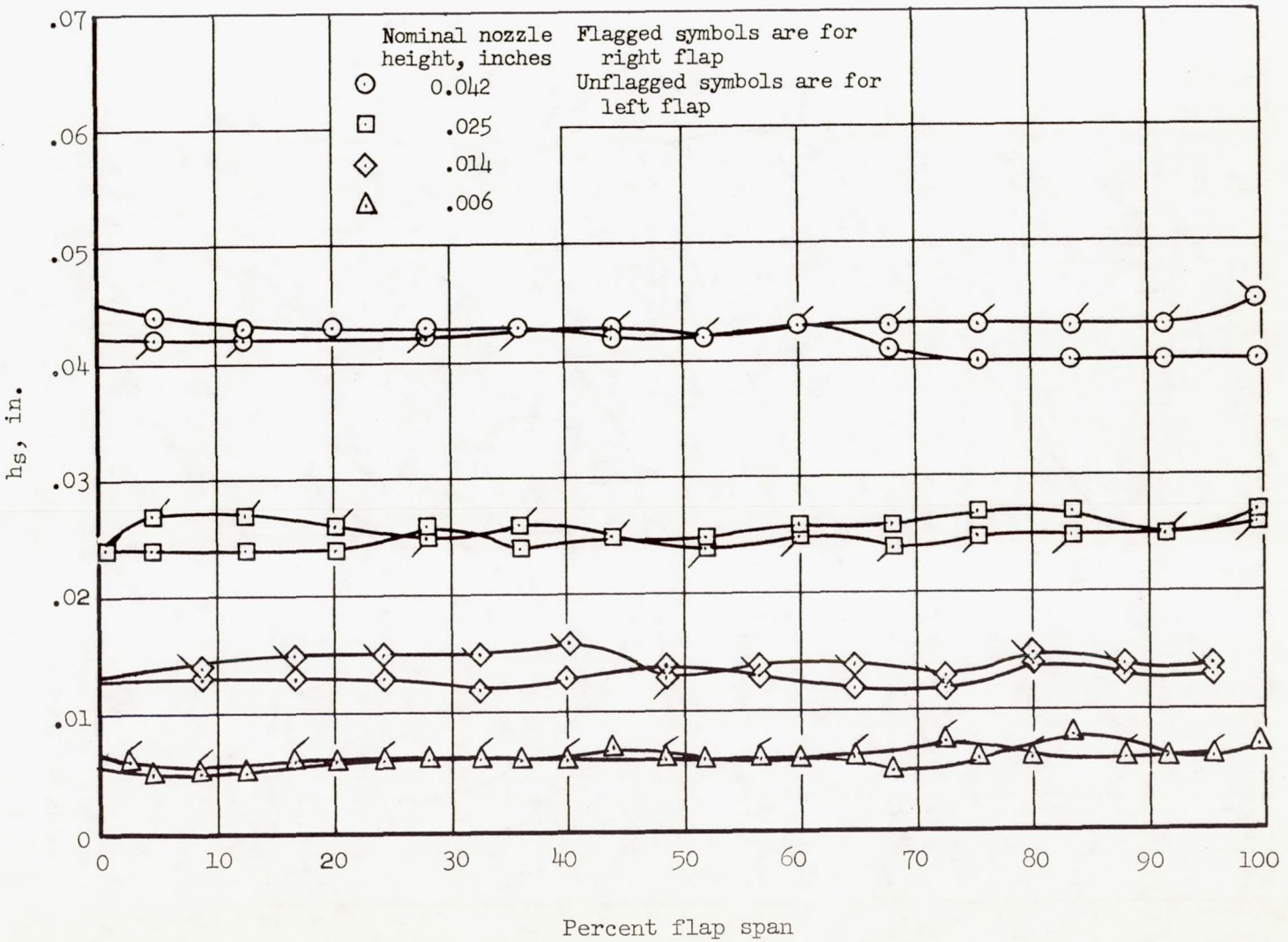

Figure 4.- Spanwise variation of flap nozzle height at ambient pressure and temperature.

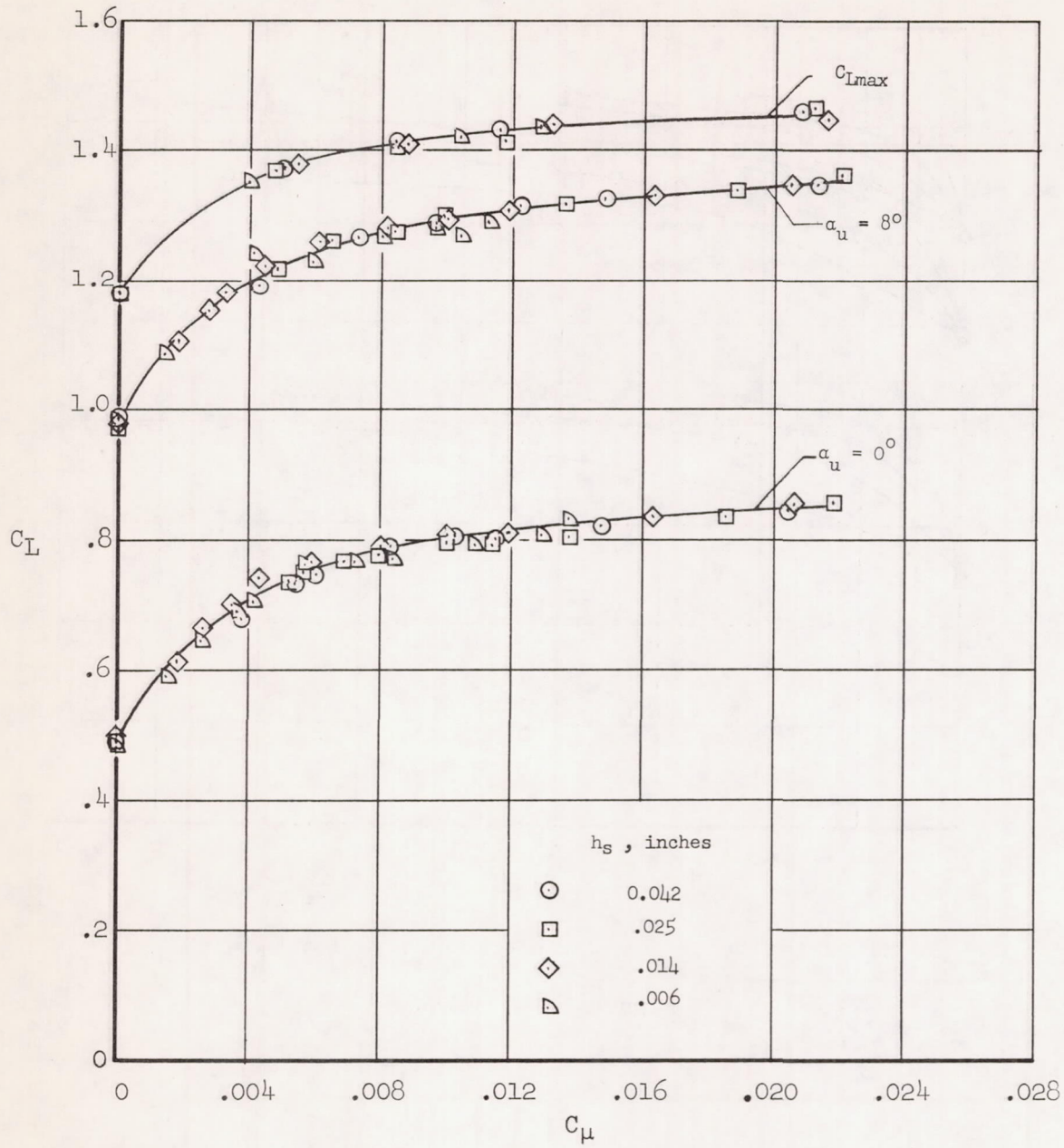

(a) Variation of C_L with C_μ.

Figure 5.- Effect of nozzle height on flow requirements of the boundary-layer control system; $\delta_f = 60^\circ$, $R = 10.7 \times 10^6$.

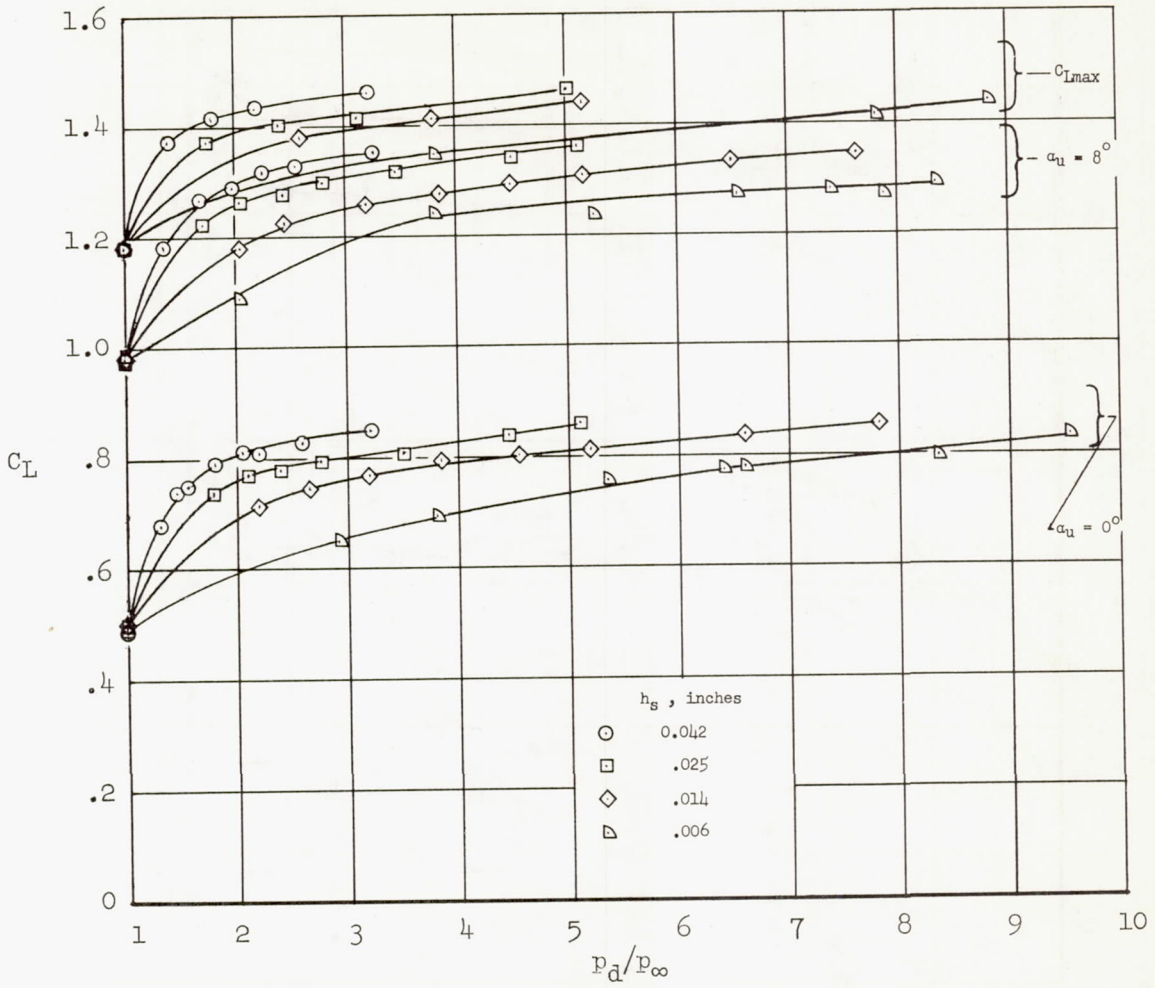

(b) Variation of C_L with pressure ratio; $\delta_f = 60^\circ$.

Figure 5.- Continued.

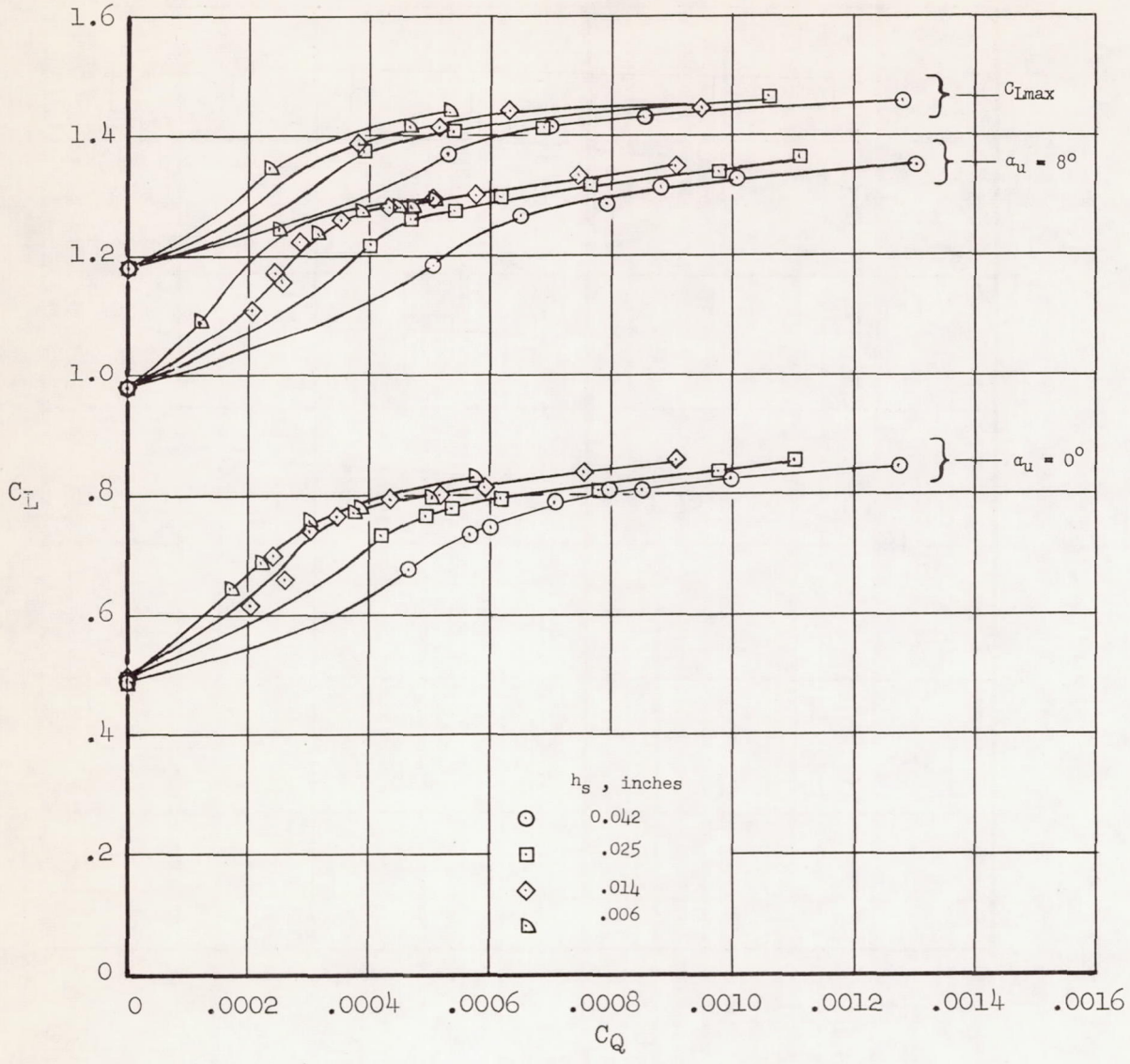

(c) Variation of C_L with C_Q; $\delta_f = 60°$.

Figure 5.- Concluded.

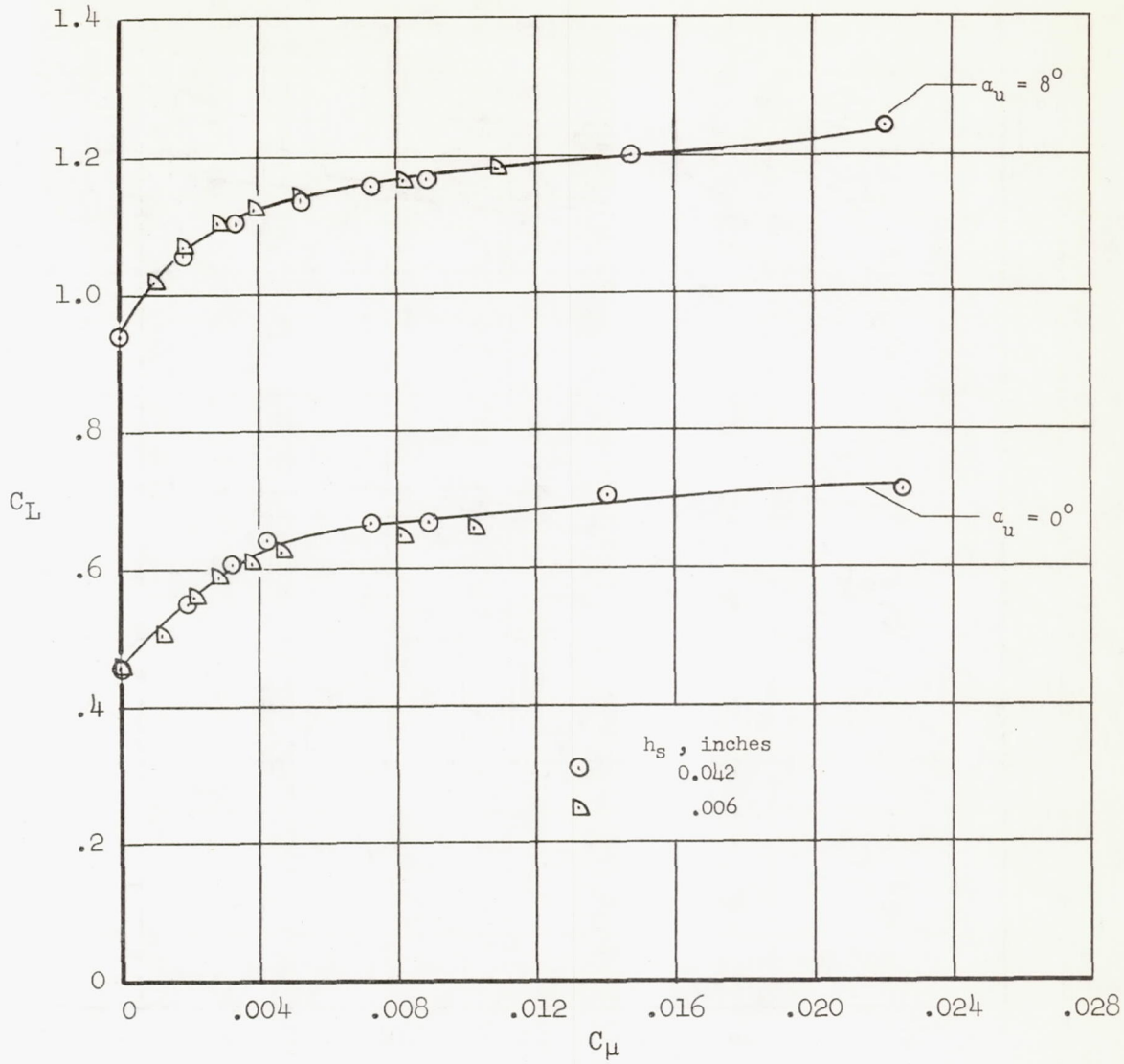

(a) Variation of C_L with C_μ.

Figure 6.- Effect of nozzle height on flow requirements of the boundary-layer control system; $\delta_f = 45°$, $R = 10.7 \times 10^6$.

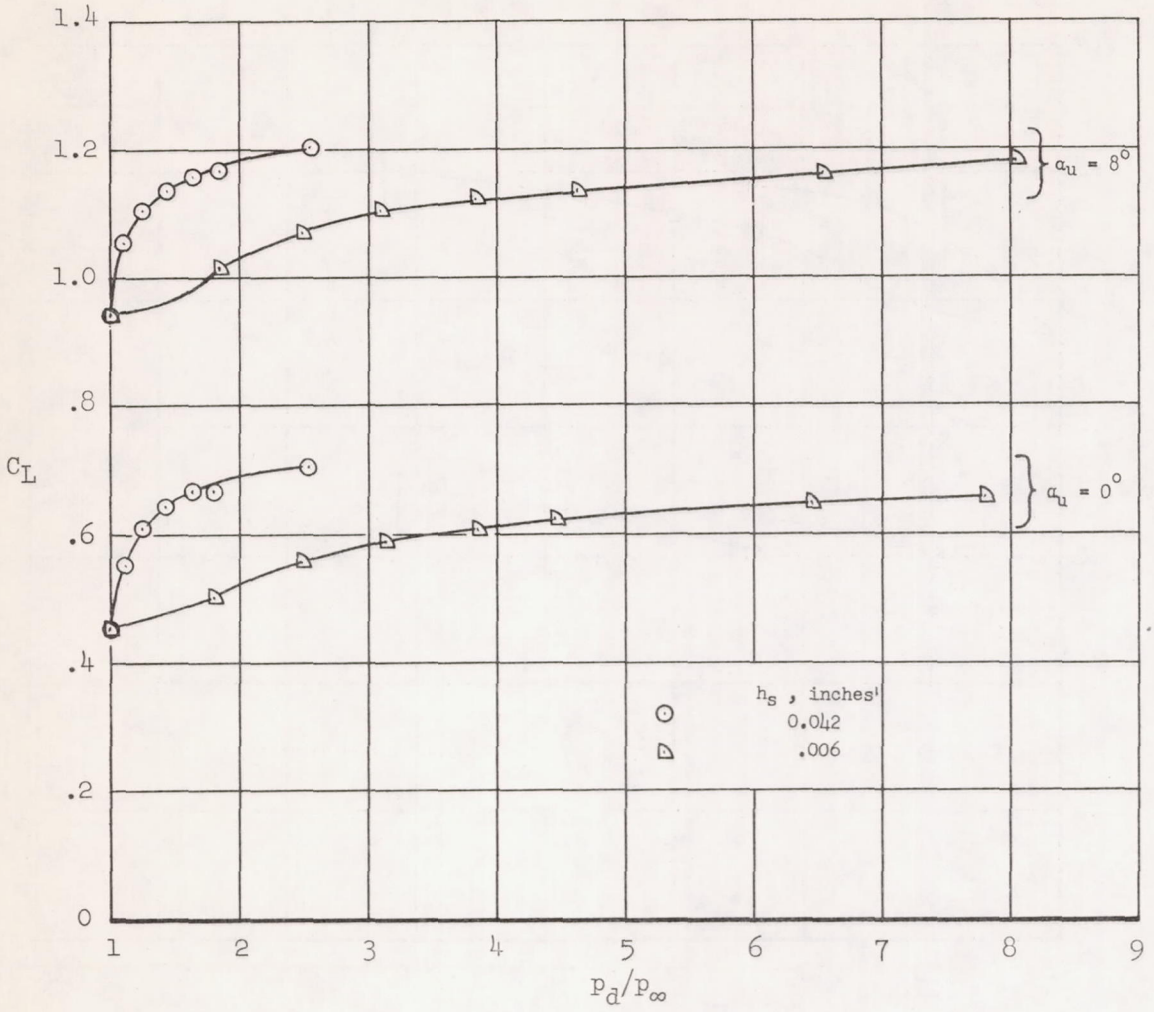

(b) Variation of C_L with pressure ratio; $\delta_f = 45^\circ$.

Figure 6.- Continued.

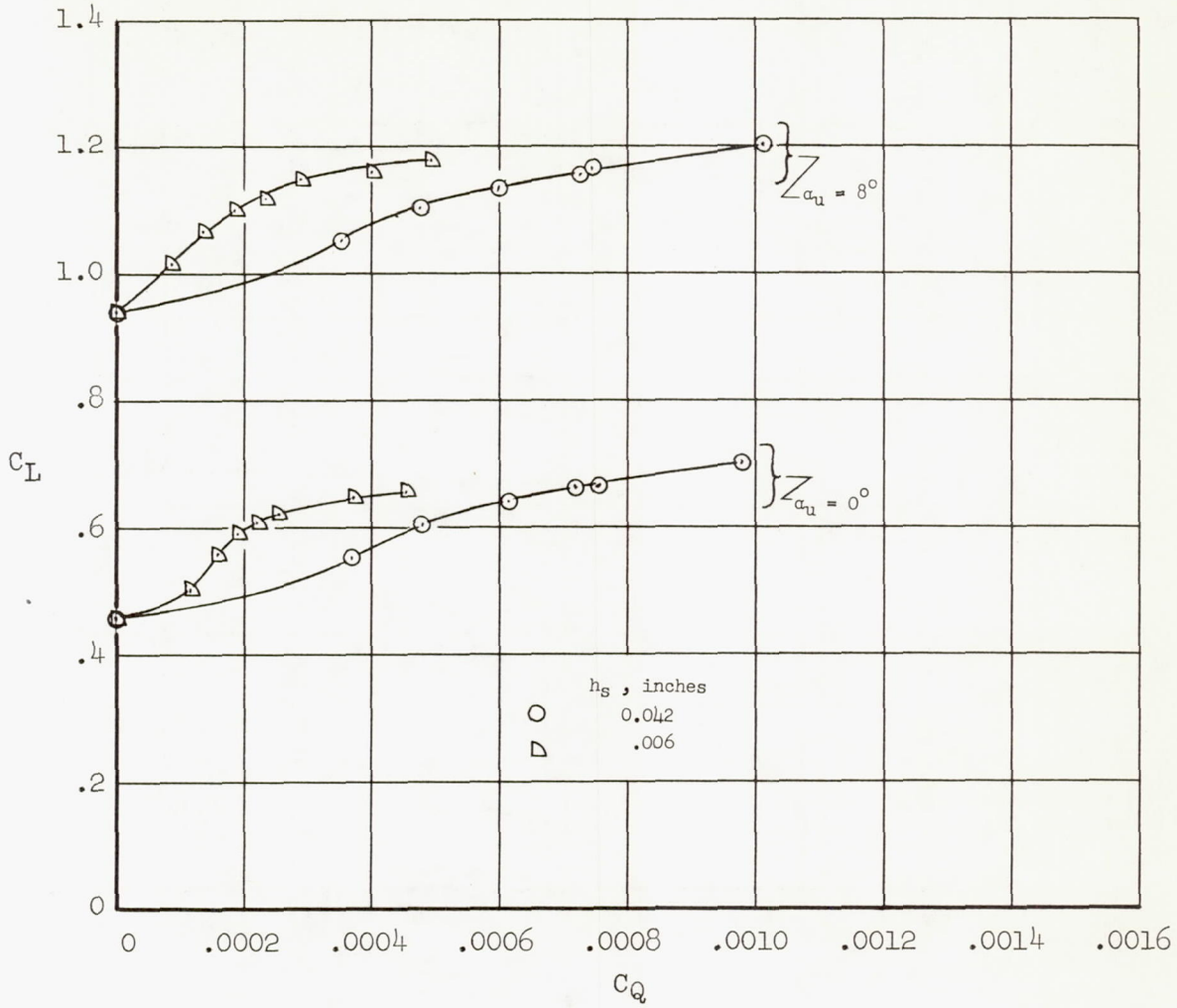

(c) Variation of C_L with C_Q; $\delta_f = 45°$.

Figure 6.- Concluded.

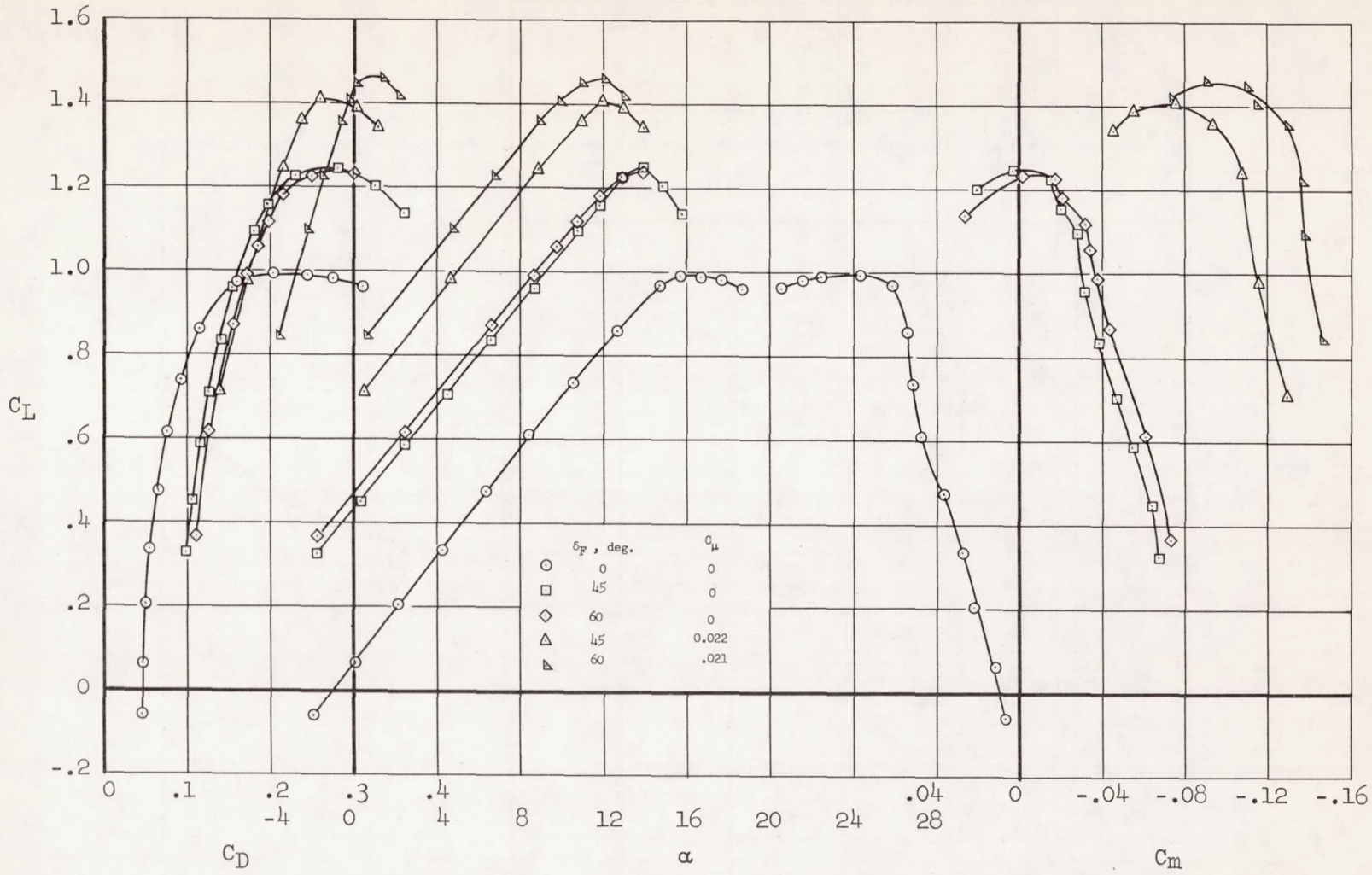

Figure 7.- Typical aerodynamic characteristics of the airplane with and without blowing; $R = 10.7 \times 10^6$.

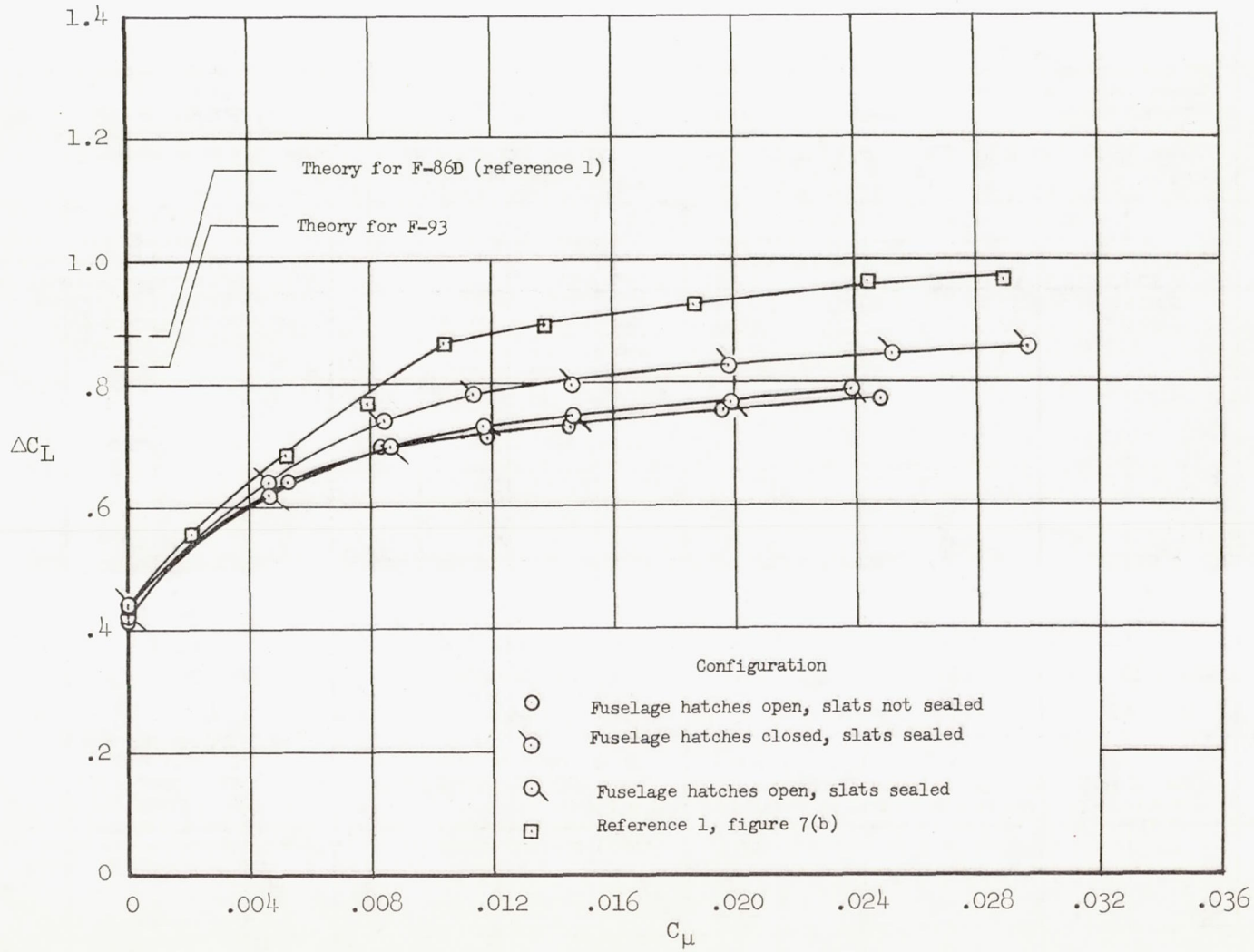

Figure 8.- Comparison of data obtained from this investigation with those obtained from reference 1 and with theory; $\delta_f = 60^\circ$, $R = 7.6 \times 10^6$, $\alpha_u = 0$.

NACA - Langley Field, Va.